We are IntechOpen, the world's leading publisher of Open Access books Built by scientists, for scientists

6,900
Open access books available

186,000
International authors and editors

200M
Downloads

Our authors are among the

154
Countries delivered to

TOP 1%
most cited scientists

12.2%
Contributors from top 500 universities

WEB OF SCIENCE™

Selection of our books indexed in the Book Citation Index in Web of Science™ Core Collection (BKCI)

Interested in publishing with us?
Contact book.department@intechopen.com

Numbers displayed above are based on latest data collected.
For more information visit www.intechopen.com

6

A Robust Iterative Multiframe SRR based on Hampel Stochastic Estimation with Hampel-Tikhonov Regularization

Vorapoj Patanavijit
Faculty of Engineering, Assumption University, Bangkok, 10240
Email: Patanavijit@yahoo.com
Thailand

Abstract

Typically, Super Resolution Reconstruction (SRR) is the process by which additional information is incorporated to enhance a noisy low resolution image hence producing a high resolution image. Although many such SRR algorithms have been proposed in the last two decades, almost SRR estimations are based on L1 or L2 statistical norm estimation therefore these SRR algorithms are usually very sensitive to their assumed model of data and noise that limits their utility. Unfortunately, the real noise models that corrupt the measure sequence are unknown; consequently, SRR algorithm using L1 or L2 norm may degrade the image sequence rather than enhance it. This paper proposes a novel SRR algorithm based on the stochastic regularization technique of Bayesian MAP estimation by minimizing a cost function. The Hampel norm is used for measuring the difference between the projected estimate of the high-resolution image and each low resolution image in order to remove outliers in the data. Moreover, Tikhonov regularization and Hampel-Tikhonov regularization are used to remove artifacts from the final answer and improve the rate of convergence. Finally, the efficiency of the proposed algorithm is demonstrated here in the experimental results using the Lena (Standard Image) and the Susie (40th Frame: Standard Sequence) in both subjective and objective measurement. The numbers of experimental results confirm the effectiveness of our method and demonstrate its superiority to other super-resolution algorithms based on L1 and L2 norm for a several noise models (such as noiseless, AWGN, Poisson, Salt & Pepper Noise and Speckle Noise) and several noise power.

1. Introduction

Super Resolution Reconstruction (SRR) traditionally allows the recovery of a high-resolution (HR) image from several low-resolution (LR) images that are noisy, blurred, and down sampled. Thus, SRR have a variety of applications in remote sensing, video frame freezing,

medical diagnostics and military information acquisition. Consequently, SRR has emerged as an alternative for producing one or a set of HR images from a sequence of LR images.
In the section, we will concentrate on the regularized reconstruction point of view therefore the estimation is one of the most important parts of the SRR algorithms and directly affect to the SRR performance. R. R. Schultz et al. (Schultz, R. R. and Stevenson R. L. 1994; Schultz, R. R. and Stevenson R. L. 1996) proposed the SRR algorithm using ML estimator (L2 Norm) with HMRF Regularization in 1996. In 1997, M. Elad et al. (Elad, M. and Feuer, A. 1997) proposed the SRR algorithm using the ML estimator (L2 Norm) with nonellipsoid constraints. Next, M. Elad et al. (Elad, M. and Feuer, A. 1999a; Elad, M. and Feuer, A. 1999c) proposed the SRR algorithm using R-SD and R-LMS (L2 Norm) in 1999. M. Elad et al. (Elad, M. and Hecov Hel-Or, Y. 2001) proposed the fast SRR algorithm ML estimator (L2 Norm) for restoration the warps are pure translations, the blur is space invariant and the same for all the images, and the noise is i.i.d. Gaussian in 2001. A. J. Patti et al. proposed (Patti, A. J. and Altunbasak, Y. 2001) a SRR algorithm using ML (L2 Norm) estimator with POCS-based regularization in 2001 and Y. Altunbasak et al. (Altunbasak, Y., Patti, A. J. and Mersereau, R. M. 2002) proposed a SRR algorithm using ML (L2 Norm) estimator for the MPEG sequences in 2002. D. Rajan et al. (Rajan, D., Chaudhuri, S. and Joshi, M. V. 2003, Rajan, D. and Chaudhuri, S. 2003) proposed SRR using ML (L2 Norm) with MRF regularization to simultaneously estimate the depth map and the focused image of a scene in 2003. S. Farsiu et al. (Farsiu, S., Robinson, M. D., Elad, M., Milanfar, P. 2004; Farsiu, S., Robinson, M. D., Elad, M. and Milanfar, P. 2004) proposed SRR algorithm ML estimator (L1 Norm) with BTV Regularization in 2004. Next, they propose a fast SRR of color images (Farsiu, S., Elad, M. and Milanfar, P. 2006) using ML estimator (L1 Norm) with BTV and Tikhonov Regularization in 2006. Y. He et at. (He, Y., Yap, K., Chen, L. and Lap-Pui 2007) proposed SRR algorithm to integrate image registration into SRR estimation (L2 Norm) in 2007. For the data fidelity cost function, all the above SRR methods are based on the simple estimation techniques such as L1 Norm or L2 Norm Minimization. For normally distributed data, the L1 norm produces estimates with higher variance than the optimal L2 (quadratic) norm but the L2 norm is very sensitive to outliers because the influence function increases linearly and without bound. From the robust statistical estimation (Black, M. J. and Rangarajan, A. 1996), Hampel Norm is designed to be more robust than L1 and L2. Hampel norm is designed to be robustness and reject outliers, the norm must be more forgiving about outliers; that is, it should increase less rapidly than L2. This paper proposes a robust iterative SRR algorithm using Hampel norm for the data fidelity cost function with Tikhonov Regularization and Hampel-Tikhonov Regularization. While the former is responsible for robustness and edge preservation, the latter seeks robustness with respect to blur, outliers, and other kinds of errors not explicitly modeled in the fused images. This experimental results demonstrate that our method's performance is superior to what was proposed earlier in this previous reviews.
The organization of this paper is as follows. Section 2 briefly introduces the main concepts of estimation technique in SRR frameworks based on L1 and L2 norm minimization. Section 3 presents the proposed SRR based on Hampel norm minimization with Tikhonov Regularization and Hampel-Tikhonov Regularization. Section 4 outlines the proposed solution and presents the comparative experimental results obtained by using the proposed Hampel norm method and by using the L1 and L2 norm method. Finally, Section 5 provides the summary and conclusion.

2. Introduction of SRR algorithms

For SRR framework (Elad, M. and Feuer, A. 1999b, Elad, M. and Hecov Hel-Or, Y. 2001), Assume that low-resolution frames of images are $\{\mathbf{Y}(t)\}$ as our measured data and each frame contains $N_1 \times N_2$ pixels. A high-resolution frame $\mathbf{X}(t)$ is to be estimated from the N low-resolution images and each frame contains $qN_1 \times qN_2$ pixels, where q is an integer-valued interpolation factor in both the horizontal and vertical directions. To reduce the computational complexity, each frame is separated into overlapping blocks. For convenience of notation, all overlapping blocked frames will be presented as vector, ordered column-wise lexicographically. Namely, the overlapping blocked LR frame is $\underline{Y}_k \in \mathbb{R}^{M^2}$ $(M^2 \times 1)$ and the overlapping blocked HR frame is $\underline{X} \in \mathbb{R}^{q^2M^2}$ $(L^2 \times 1 \text{ or } q^2M^2 \times 1)$. We assume that the two images are related via the following equation

$$\underline{Y}_k = D_k H_k F_k \underline{X} + \underline{V}_k \quad ;k = 1,2,\ldots,N \tag{1.1}$$

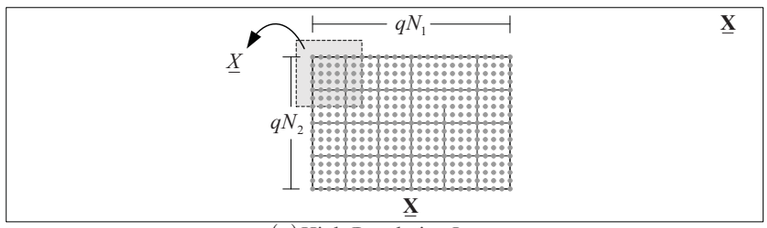

(a) High-Resolution Image

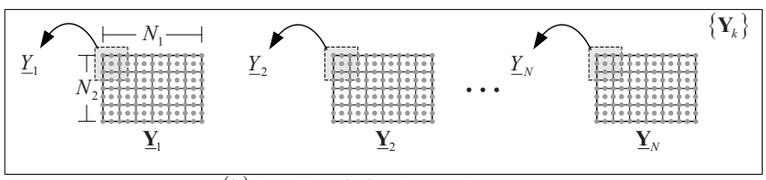

(b) Low-Resolution Image Sequence

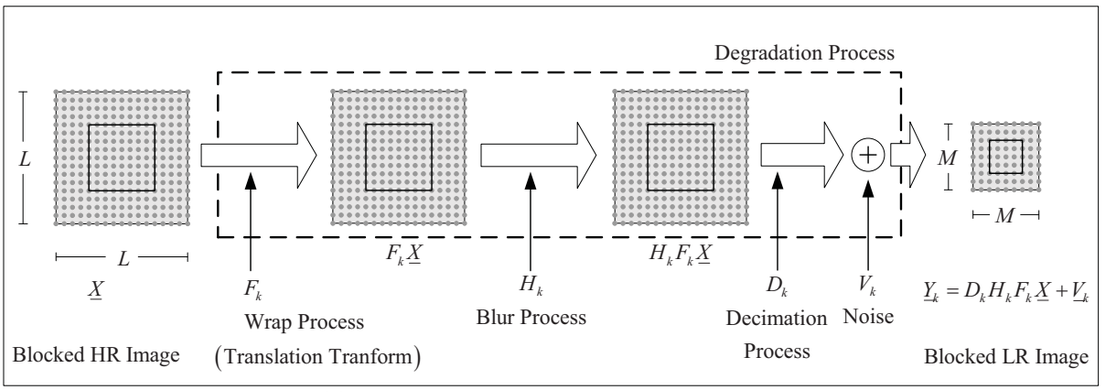

(c) The Relation between Overlapping Blocked HR Image
and Overlapping Blocked LR Image Sequence
(SRR Observation Model)

Fig. 1. The Classical SRR Observation Model

where

- $\underline{X}$ (vector format) is the original high-resolution blocked image.
- $\underline{Y}_k(t)$ (vector format) is the blurred, decimated, down sampled and noisy blocked image
- F_k ($F \in \mathbb{R}^{q^2M^2 \times q^2M^2}$ and matrix format) stands for the geometric warp (Typically, Translational Motion) between the images $\underline{X}$ and $\underline{Y}_k$.
- H_k ($H_k \in \mathbb{R}^{q^2M^2 \times q^2M^2}$ and matrix format)is the blur matrix which is a space and time invariant.
- D_k ($D_k \in \mathbb{R}^{M^2 \times q^2M^2}$ and matrix format) is the decimation matrix assumed constant.
- $\underline{V}_k$ ($\underline{V}_k \in \mathbb{R}^{M^2}$ and vector format) is a system noise.

A popular family of estimators is the ML-type estimators (M estimators) (Elad, M. and Feuer, A. 1999c). We rewrite the definition of these estimators in the super resolution reconstruction framework as the following minimization problem:

$$\underline{\hat{X}} = \underset{\underline{X}}{\text{ArgMin}} \left\{ \sum_{k=1}^{N} \rho\left(D_k H_k F_k \underline{X} - \underline{Y}_k \right) \right\} \tag{1.2}$$

where $\rho(\cdot)$ is a norm estimation. To minimize (1.2), the intensity at each pixel of the expected image must be close to those of the original image.

SRR (Super-Resolution Reconstruction) is an ill-posed problem (Elad, M. and Feuer, A. 1997; Elad, M. and Feuer, A. 1999a; Elad, M. and Feuer, A. 1999b; Elad, M. and Hecov Hel-Or, Y. 2001; Elad, M. and Feuer, A. 1999c). For the under-determined cases (i.e., when fewer than required frames are available), there exist an infinite number of solutions which satisfy (1.2). The solution for squared and over-determined cases is not stable, which means small amounts of noise in measurements will result in large perturbations in the final solution. Therefore, considering regularization in SRR algorithm as a mean for picking a stable solution is very useful, if not necessary. Also, regularization can help the algorithm to remove artifacts from the final answer and improve the rate of convergence. A regularization term compensates the missing measurement information with some general prior information about the desirable HR solution, and is usually implemented as a penalty factor in the generalized minimization cost function. Unfortunately, certain types of regularization cost functions work efficiently for some special types of images but are not suitable for general images.

2.1 L1 Norm with Tikhonov Regularization

A popular family of estimators is the L1 Norm estimators that are used in SRR problem (Farsiu, S., Robinson, M. D., Elad, M. and Milanfar, P. 2004; Farsiu, S., Elad, M. and Milanfar, P. 2006). Due to ill-posed problem of SRR, a regularization term compensates the missing measurement information with some general prior information about the desirable HR solution, and is usually implemented as a penalty factor in the generalized minimization cost function. The most classical and simplest Tikhonov regularization cost functions is the

Laplacian regularization (Farsiu, S., Robinson, M. D., Elad, M. and Milanfar, P. 2004) therefore we rewrite the definition of these estimators in the SRR context as the following minimization problem:

$$\underline{X} = \underset{\underline{X}}{\text{ArgMin}} \left\{ \sum_{k=1}^{N} \left\| D_k H_k F_k \underline{X} - \underline{Y}_k \right\| + \lambda \cdot \left(\Gamma \underline{X} \right)^2 \right\} \tag{2}$$

where the Laplacian kernel (Farsiu, S., Robinson, M. D., Elad, M. and Milanfar, P. 2004) is defined as

$$\Gamma = 1/8 \begin{bmatrix} 1 & 1 & 1 \; ; & 1 & -8 & 1 \; ; & 1 & 1 & 1 \end{bmatrix} \tag{3}$$

By the steepest descent method, the solution is:

$$\underline{\hat{X}}_{n+1} = \underline{\hat{X}}_n + \beta \cdot \left\{ \begin{array}{l} \left(\sum_{k=1}^{N} F_k^T H_k^T D_k^T \operatorname{sign}\left(D_k H_k F_k \underline{\hat{X}}_n - \underline{Y}_k \right) \right) \\ -\left(\lambda \cdot \left(\Gamma^T \Gamma \right) \underline{\hat{X}}_n \right) \end{array} \right\} \tag{4}$$

where β is the step size in the gradient direction.

2.2 L2 Norm with Tikhonov Regularization

Another popular family of estimators is the L2 Norm estimators that are used in SRR problem (Schultz, R. R. and Stevenson R. L. 1994; Schultz, R. R. and Stevenson R. L. 1997). We rewrite the definition of these estimators in the SRR context that is combined the Laplacian regularization as the following minimization problem:

$$\underline{X} = \underset{\underline{X}}{\text{ArgMin}} \left\{ \sum_{k=1}^{N} \left\| D_k H_k F_k \underline{X} - \underline{Y}_k \right\|_2^2 + \lambda \cdot \left(\Gamma \underline{X} \right)^2 \right\} \tag{5}$$

By the steepest descent method, the solution is:

$$\underline{\hat{X}}_{n+1} = \underline{\hat{X}}_n + \beta \cdot \left\{ \begin{array}{l} \sum_{k=1}^{N} F_k^T H_k^T D_k^T \left(\underline{Y}_k - D_k H_k F_k \underline{\hat{X}}_n \right) \\ -\left(\lambda \cdot \left(\Gamma^T \Gamma \right) \underline{\hat{X}}_n \right) \end{array} \right\} \tag{6}$$

3. The Proposed Robust SRR Algorithm

The success of SRR algorithm is highly dependent on the accuracy of the imaging process model. Unfortunately, these models are not supposed to be exactly true, as they are merely mathematically convenient formulations of some general prior information. When the data or noise model assumptions do not faithfully describe the measure data, the estimator

performance degrades. Furthermore, existence of outliers defined as data points with different distributional characteristics than the assumed model will produce erroneous estimates. Almost all noise models used in SRR algorithms are based on Additive White Gaussian Noise (AWGN) model; therefore, SRR algorithms can effectively apply only on the image sequence that is corrupted by AWGN. Due to this noise model, L1 norm or L2 norm error are effectively used in SRR algorithm. Unfortunately, the real noise models that corrupt the measure sequence are unknown therefore SRR algorithm using L1 norm or L2 norm may degrade the image sequence rather than enhance it. The robust norm error is necessary for SRR algorithm applicable to several noise models. For normally distributed data, the L1 norm produces estimates with higher variance than the optimal L2 (quadratic) norm but the L2 norm is very sensitive to outliers because the influence function increases linearly and without bound. From the robust statistical estimation (Black, M. J. and Rangarajan, A. 1996), Hampel Norm is designed to be more robust than L1 and L2. While these robust norms are designed to reject outliers, these norms must be more forgiving about the remaining outliers; that is, it should increase less rapidly than L2.

A robust estimation is estimated technique that is resistance to such outliers. In SRR framework, outliers are measured images or corrupted images that are highly inconsistent with the high resolution original image. Outliers may arise from several reasons such as procedural measurement error, noise or inaccurate mathematical model. Outliers should be investigated carefully; therefore, we need to analyze the outlier in a way which minimizes their effect on the estimated model. L2 norm estimation is highly susceptible to even a small number of discordant observations or outliers. For L2 norm estimation, the influence of the outlier is much larger than the other measured data because L2 norm estimation weights the error quadraticly. Consequently, the robustness of L2 norm estimation is poor.

Hampel's norm (Black, M. J. and Rangarajan, A. 1996) is one of error norm from the robust statistic literature. It is equivalent to the L1 norm for large value. But, for normally distributed data, the L1 norm produces estimates with higher variance than the optimal L2 (quadratic) norm, so Hampel's norm is designed to be quadratic for small values and its influence does not descend all the way to zero. The Hampel norm function ($\rho(\cdot)$) and its influence function ($\rho'(\cdot)$) are shown in Figure 2.1 (a) and Figure 2.1 (b), respectively

We rewrite the definition of these estimators in the super resolution context as the following minimization problem:

$$\underline{X} = \underset{\underline{X}}{\text{ArgMin}} \left\{ \sum_{k=1}^{N} f_{HAMPEL} \left(D_k H_k F_k \underline{X} - \underline{Y}_k \right) \right\} \tag{7}$$

By the steepest descent method, the solution is:

$$f_{HAMPEL}(x) = \begin{cases} x^2 & ;|x| \le T \\ 2T|x| - T^2 & ;T < |x| \le 2T \\ 4T^2 - \left(3T - |x|\right)^2 & ;2T < |x| \le 3T \\ 4T^2 & ;|x| > 3T \end{cases} \tag{8}$$

where T is Hampel constant parameter.

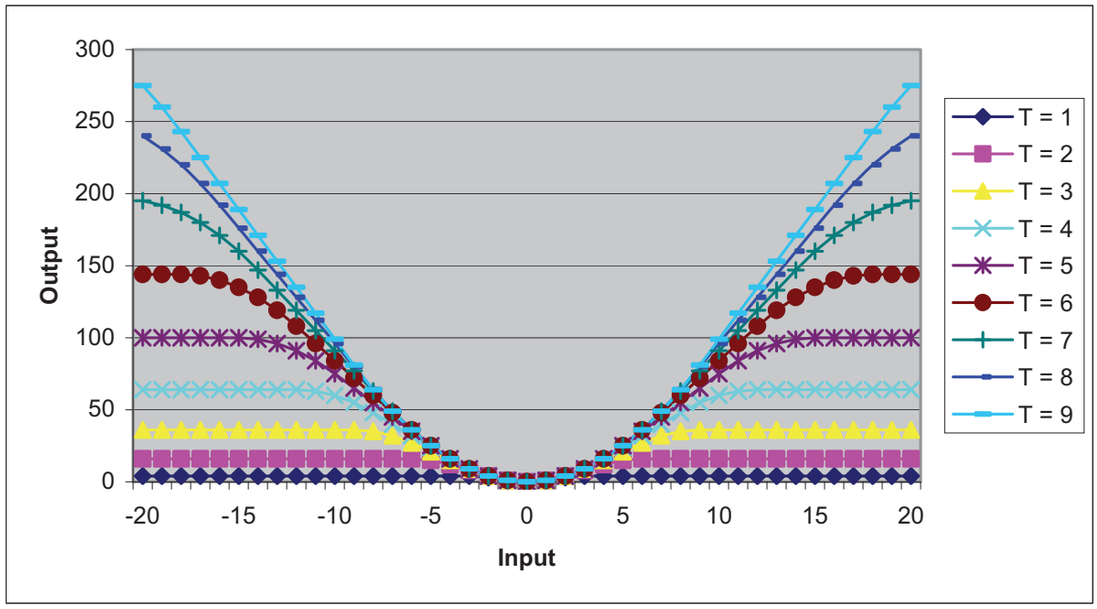

Fig. 2(a). The Hampel Norm function

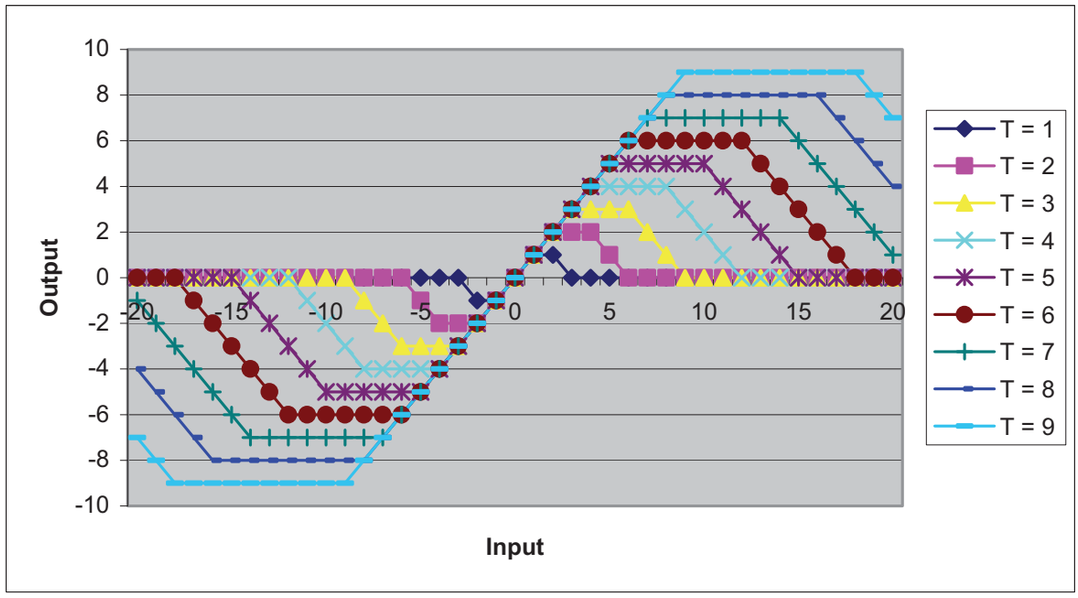

Fig. 2(b). The Influence function of Hampel Norm

3.1 Hampel Norm with Tikhonov Regularization

The most classical and simplest Tikhonov regularization cost functions is the Laplacian regularization (Farsiu, S., Robinson, M. D., Elad, M. and Milanfar, P. 2004) therefore we rewrite the definition of these estimators in the SRR context as the following minimization problem:

$$\underline{X} = \underset{\underline{X}}{\text{ArgMin}} \left\{ \sum_{k=1}^{N} f_{HAMPEL}\left(D_k H_k F_k \underline{X} - \underline{Y}_k\right) + \lambda \cdot \left(\Gamma \underline{X}\right)^2 \right\} \tag{9}$$

By the steepest descent method, the solution is:

$$\hat{\underline{X}}_{n+1} = \hat{\underline{X}}_n + \beta \cdot \left\{ \begin{array}{l} \sum_{k=1}^{N} F_k^T H_k^T D_k^T \cdot \psi_{HAMPEL}\left(\underline{Y}_k - D_k H_k F_k \hat{\underline{X}}_n\right) \\ -\left(\lambda \cdot \left(\Gamma^T \Gamma\right) \hat{\underline{X}}_n\right) \end{array} \right\} \tag{10}$$

$$\psi_{HAMPEL}(x) = f'_{HAMPEL}(x) = \begin{cases} 2x & ;|x| \le T \\ 2T \operatorname{sign}(x) & ;T < |x| \le 2T \\ 2\left(3T - |x|\right)\operatorname{sign}(x) & ;2T < |x| \le 3T \\ 0 & ;|x| > 3T \end{cases} \tag{11}$$

3.2 Hampel Norm with Hampel-Tikhonov Regularization

This paper proposes an alternative robust regularization function, so called Hampel-Tikhonov regularization, for incorporating in the SRR algorithm. Consequently, we rewrite the definition of these estimators in the SRR context combining with the Hampel-Laplacian regularization as the following minimization problem:

$$\underline{X} = \underset{\underline{X}}{\text{ArgMin}} \left\{ \sum_{k=1}^{N} f_{HAMPEL}\left(D_k H_k F_k \underline{X} - \underline{Y}_k\right) + \lambda \cdot g_{HAMPEL}\left(\Gamma \underline{X}\right) \right\} \tag{12}$$

$$g_{HAMPEL}(x) = \begin{cases} x^2 & ;|x| \le T_g \\ 2T_g |x| - {T_g}^2 & ;T_g < |x| \le 2T_g \\ 4{T_g}^2 - \left(3T_g - |x|\right)^2 & ;2T_g < |x| \le 3T_g \\ 4{T_g}^2 & ;|x| > 3T_g \end{cases} \tag{13}$$

By the steepest descent method, the solution is:

$$\hat{\underline{X}}_{n+1} = \hat{\underline{X}}_n + \beta \cdot \left\{ \begin{array}{l} \sum_{k=1}^{N} F_k^T H_k^T D_k^T \cdot \psi_{HAMPEL}\left(\underline{Y}_k - D_k H_k F_k \hat{\underline{X}}_n\right) \\ -\left(\lambda \cdot \Gamma^T \cdot \zeta_{HAMPEL}\left(\Gamma \hat{\underline{X}}_n\right)\right) \end{array} \right\} \tag{14}$$

$$\zeta_{HAMPEL}(x) = g'_{HAMPEL}(x) = \begin{cases} 2x & ;|x| \le T_g \\ 2T_g \operatorname{sign}(x) & ;T_g < |x| \le 2T_g \\ 2\left(3T_g - |x|\right)\operatorname{sign}(x) & ;2T_g < |x| \le 3T_g \\ 0 & ;|x| > 3T_g \end{cases} \tag{15}$$

4. Experimental Result

This section presents the experiments and results obtained by the proposed robust SRR methods using Hampel norm with Tikhonov regularization and with Hampel- Tikhonov regularization that are calculated by (10-11) and (14-15) respectively. To demonstrate the proposed robust SRR performance, the results of L1 norm SRR (Farsiu, S., Robinson, M. D., Elad, M. and Milanfar, P. 2004; Farsiu, S., Elad, M. and Milanfar, P. 2006) with Laplacian regularization that is calculated by (4) and the results of L2 norm SRR (Schultz, R. R. and Stevenson R. L. 1994; Schultz, R. R. and Stevenson R. L. 1997) with Laplacian regularization that is calculated by (6) are presented in order to compare the performance.
These experiments are implemented in MATLAB and the block size is fixed at 8x8 (16x16 for overlapping block). In this experiment, we create a sequence of LR frames by using the Lena (Standard Image) and Susie (40th Frame: Standard Sequence). First, we shifted this HR image by a pixel in the vertical direction. Then, to simulate the effect of camera PSF, this shifted image was convolved with a symmetric Gaussian low-pass filter of size 3x3 with standard deviation equal to one. The resulting image was subsampled by the factor of 2 in each direction. The same approach with different motion vectors (shifts) in vertical and horizontal directions was used to produce 4 LR images from the original scene. We added difference noise model to the resulting LR frames. Next, we use 4 LR frames to generate the high resolution image by the different SRR methods.
The criterion for parameter selection in this paper was to choose parameters which produce both most visually appealing results and highest PSNR. Therefore, to ensure fairness, each experiment was repeated several times with different parameters and the best result of each experiment was chosen (Farsiu, S., Robinson, M. D., Elad, M. and Milanfar, P. 2004; Farsiu, S., Elad, M. and Milanfar, P. 2006).
For objective or PSNR measurement of the Lena (Standard image) and Susie (40th Frame) are shown in Table I and Table II respectively. For subjective or virtual measurement of the Lena (Standard image) and Susie (40th Frame) are shown in figure 3 and figure 4 respectively.

4.1 Noiseless

For objective or PSNR measurement, the result of the Lena (Standard image) and Susie (40th Frame) are shown in Table I and II respectively. The result of SRR based on Hampel estimator with Laplacian and Hampel-Laplacian Regularization gives outstandingly higher PSNR than L1 and L2 norm estimator about 1-3 dB.
For subjective or virtual measurement of Lena (Standard image), the original HR image is shown in Fig. 3 (a-1) and one of corrupted LR images is shown in Fig. 3 (a-2). Next, the result of implementing the SRR algorithm using L1 estimator with Laplacian Regularization, L2 estimator with Laplacian Regularization, Hampel estimator with Laplacian Regularization and Hampel estimator with Hampel-Laplacian Regularization are shown in Figs. 3 (a-3) – 3 (a-6) respectively.
For subjective or virtual measurement of Susie (40th Frame), the original HR image is shown in Fig. 4 (a-1) and one of corrupted LR images is shown in Fig. 4 (a-2). Next, the result of implementing the SRR algorithm using L1 estimator with Laplacian Regularization, L2 estimator with Laplacian Regularization, Hampel estimator with Laplacian Regularization

and Hampel estimator with Hampel-Laplacian Regularization are shown in Figs. 4 (a-3) – 4 (a-6) respectively.

Noise Model	The PSNR of SRR Image (dB)				
	LR Image	L1 with Reg	L2 with Reg	Hamp. with Reg	Hamp. with H-Reg
Noiseless	28.8634	28.8634	30.8553	31.4877 T=19	31.4877 T=19 Tg=19
AWGN (dB): SNR=25	27.8884	27.949	29.6579	29.7453 T=19	29.7453 T=19 Tg=5
SNR=22.5	27.2417	27.4918	29.1611	29.1916 T=19	29.1923 T=19 Tg=9
SNR=20	26.2188	26.7854	28.6024	28.6089 T=19	28.6095 T=19 Tg=15
SNR=17.5	24.9598	26.0348	27.8153	27.8186 T=19	27.8186 T=19 Tg=19
SNR=15	23.3549	25.1488	26.6406	26.6117 T=19	26.6117 T=19 Tg=19
Poisson	26.5116	26.9604	28.719	28.713 T=19	28.7142 T=19 Tg=9
Salt&Pepper: D=0.005	26.8577	27.1149	28.8495	30.9745 T=9	30.9745 T=9 Tg=5
D=0.010	25.2677	26.0569	28.0346	30.9721 T=9	30.9721 T=15 Tg=19
D=0.015	24.219	25.3534	27.3188	30.9652 T=9	30.9652 T=15 Tg=19
Speckle: V=0.03	23.5294	25.3133	26.6956	26.1051 T=19	26.1051 T=19 Tg=19
V=0.05	21.7994	24.4215	25.3165	25.2729 T=1	25.3542 T=1 Tg=19

Table 1. The experimental Result of Proposed Method (Lena Image)

4.2 AWGN (Additive White Gaussian Noise)

For objective or PSNR measurement, the result of the Lena (Standard image) and Susie (40th Frame) are shown in Table I and II respectively. For the Lena image, the result of SRR based on Hampel estimator with Laplacian and Hampel-Laplacian Regularization gives the higher PSNR than L1 and L2 norm estimator. For the Susie image, the result of SRR based on Hampel estimator with Laplacian and Hampel-Laplacian Regularization and L2 estimator gives the higher PSNR than L1 norm estimator.

For subjective or virtual measurement of Lena (Standard image) at 5 AWGN cases, the original HR image is shown in Fig. 3 (b-1) - 3 (f-1) respectively and one of corrupted LR images is shown in Fig. 3 (b-2) - 3 (f-2) respectively. Next, the result of implementing the SRR algorithm using L1 estimator with Laplacian Regularization, L2 estimator with Laplacian Regularization, Hampel estimator with Laplacian Regularization and Hampel estimator with Hampel-Laplacian Regularization are shown in Figs. 3 (b-3) – 3 (b-6), Figs. 3(c-3) – 3 (c-6), Figs. 3 (d-3) – 3 (d-6), Figs. 3 (e-3) – 3 (e-6) and Figs. 3 (f-3) – 3 (f-6) respectively.

For subjective or virtual measurement of Susie (40th Frame) at 3 AWGN cases, the original HR image is shown in Fig. 4 (b-1) - 4 (f-1) respectively and one of corrupted LR images is shown in Fig. 4 (b-2) - 4 (f-2) respectively. Next, the result of implementing the SRR algorithm using L1 estimator with Laplacian Regularization, L2 estimator with Laplacian Regularization, Hampel estimator with Laplacian Regularization and Hampel estimator with Hampel-Laplacian Regularization are shown in Figs. 4 (b-3) – 4 (b-6), Figs. 4 (c-3) – 4 (c-6), Figs. 4 (d-3) – 4 (d-6), Figs. 4 (e-3) – 4 (e-6) and Figs. 4 (f-3) – 4 (f-6) respectively.

Noise Model	The PSNR of SRR Image (dB)				
	LR Image	L1 with Reg	**L2 with Reg**	**Hamp. with Reg**	**Hamp. with H-Reg**
Noiseless	32.1687	32.1687	34.2	34.747 T=19	34.747 T=19
AWGN (dB): SNR=20	27.5316	28.7003	30.6898	30.6642 T=19	30.6655 T=19 Tg=19
SNR=17.5	25.7322	27.5771	29.3375	29.3112 T=19	29.3112 T=19 Tg=19
SNR=15	23.7086	26.2641	27.6671	27.6565 T=1	27.6565 T=1 Tg=19
Poisson	27.9071	28.9197	30.7634	30.7853 T=19	30.7859 T=19 Tg=19
Salt&Pepper: D=0.005	29.0649	29.5041	31.5021	34.4785 T=9	34.4785 T=9 Tg=19

D=0.010	26.4446	27.7593	29.8395	34.4803 T=9	34.4803 T=9 Tg=19
D=0.015	25.276	26.9247	28.7614	34.4483 T=9	34.4483 T=9 Tg=19
Speckle: V=0.01	27.6166	28.8289	30.6139	30.415 T=19	30.4293 T=19 Tg=9
V=0.03	24.0403	26.8165	27.7654	27.9409 T=1	28.0189 T=1 Tg=9

Table 2. The experimental Result of Proposed Method (Susie 40th Frame)

4.3 Poisson Noise

For objective or PSNR measurement, the result of the Lena (Standard image) and Susie (40th Frame) are shown in Table I and II respectively. The result of SRR based on Hampel estimator with Laplacian and Hampel-Laplacian Regularization and L2 estimator gives the higher PSNR than L1 norm estimator.

For subjective or virtual measurement of Lena (Standard image), the original HR image is shown in Fig. 3 (g-1) and one of corrupted LR images is shown in Fig. 3 (g-2). Next, the result of implementing the SRR algorithm using L1 estimator with Laplacian Regularization, L2 estimator with Laplacian Regularization, Hampel estimator with Laplacian Regularization and Hampel estimator with Hampel-Laplacian Regularization are shown in Figs. 3 (g-3) – 3 (g-6) respectively.

For subjective or virtual measurement of Susie (40th Frame), the original HR image is shown in Fig. 4 (g-1) and one of corrupted LR images is shown in Fig. 4 (g-2). Next, the result of implementing the SRR algorithm using L1 estimator with Laplacian Regularization, L2 estimator with Laplacian Regularization, Hampel estimator with Laplacian Regularization and Hampel estimator with Hampel-Laplacian Regularization are shown in Figs. 4 (g-3) – 4 (g-6) respectively

4.4 Salt&Pepper Noise

For objective or PSNR measurement, this experiment is a 3 Salt&Pepper Noise cases at D=0.005, D=0.010 and D=0.015 respectively (D is the noise density for Salt&Pepper noise model). The result of the Lena (Standard image) and Susie (40th Frame) are shown in Table I and II respectively. The result of SRR based on Hampel estimator with Laplacian and Hampel-Laplacian Regularization gives dramatically higher PSNR than L1 and L2 norm estimator about 4-5 dB.

For subjective or virtual measurement of Lena (Standard image) at 3 Salt&Pepper Noise cases, the original HR image is shown in Fig. 3 (h-1) - 3 (j-1) respectively and one of corrupted LR images is shown in Fig. 3 (h-2) - 3 (j-2) respectively. Next, the result of implementing the SRR algorithm using L1 estimator with Laplacian Regularization, L2 estimator with Laplacian Regularization, Hampel estimator with Laplacian Regularization

and Hampel estimator with Hampel-Laplacian Regularization are shown in Figs. 3 (h-3) – 3 (h-6), Figs. 3 (i-3) – 3 (i-6) and Figs. 3 (j-3) – 3 (j-6) respectively.
For subjective or virtual measurement of Susie (40th Frame) at 3 Salt&Pepper Noise cases, the original HR image is shown in Fig. 4 (h-1) - 4 (j-1) respectively and one of corrupted LR images is shown in Fig. 4 (h-2) - 4 (j-2) respectively. Next, the result of implementing the SRR algorithm using L1 estimator with Laplacian Regularization, L2 estimator with Laplacian Regularization, Hampel estimator with Laplacian Regularization and Hampel estimator with Hampel-Laplacian Regularization are shown in Figs. 4 (h-3) – 4 (h-6), Figs. 4 (i-3) – 4 (i-6) and Figs. 4 (j-3) – 4 (j-6) respectively.

4.5 Speckle Noise

For objective or PSNR measurement, the result of the Lena (Standard image) and Susie (40th Frame) are shown in Table I and II respectively. (V is the noise variance for Speckle noise model) The result of SRR based on Hampel estimator with Laplacian and Hampel-Laplacian Regularization and L2 estimator gives the higher PSNR than L1 norm estimator.
For subjective or virtual measurement of Lena (Standard image) at 2 Speckle cases, the original HR image is shown in Fig. 3 (k-1) - 3 (l-1) respectively and one of corrupted LR images is shown in Fig. 3 (k-2) - 3 (l-2) respectively. Next, the result of implementing the SRR algorithm using L1 estimator with Laplacian Regularization, L2 estimator with Laplacian Regularization, Hampel estimator with Laplacian Regularization and Hampel estimator with Hampel-Laplacian Regularization are shown in Figs. 3 (k-3) – 3 (k-6) and Figs. 3 (l-3) – 3 (l-6) respectively.
For subjective or virtual measurement of Susie (40th Frame) at 2 Speckle cases, the original HR image is shown in Fig. 4 (k-1) - 4 (m-1) respectively and one of corrupted LR images is shown in Fig. 4 (k-2) - 4 (m-2) respectively. Next, the result of implementing the SRR algorithm using L1 estimator with Laplacian Regularization, L2 estimator with Laplacian Regularization, Hampel estimator with Laplacian Regularization and Hampel estimator with Hampel-Laplacian Regularization are shown in Figs. 4 (k-3) – 4 (k-6), Figs. 4 (l-3) – 4 (l-6) and Figs. 4 (m-3) – 4 (m-6) respectively.
From the number of experimental results, the T parameter is low (like L1 norm) such as T=1 to T=5 for high noise power and is high for low noise power (like L2 norm) such as T=15 to T=19. Moreover, the T_g parameter is medium (like L1-Tikhonov regularization) for high noise power and is high for low noise power (like classical Tikhonov regularization).
The computation cost of the proposed algorithm slightly higher than the SRR algorithm based on L1 and L2.
From all experimental results of both Susie (40th Frame) and Lena (The Standard Image), all comparatively experimental results are concluded as follow:

1. For AWGN case, the L2 estimator usually gives the best reconstruction because noise distribution is a quadratic similar to L2.
2. For Salt&Pepper Noise cases, the Hampel estimator gives the far better reconstruction than L1 and L2 estimator because these robust estimators are designed to be robust and reject outliers. The norms are more forgiving on outliers; that is, they should increase less rapidly than L2.
3. The SRR algorithm using L1 norm with the proposed registration gives the lowest PSRN because the L1 norm is excessively robust against the outliers.

5. Conclusion

In this paper, we propose an alternate approach using a novel robust estimation norm function (based on Hampel norm function) for SRR framework with Tikhonov and Hampel-Tikhonov Regularization. The proposed robust SRR can be effectively applied on the images that are corrupted by various noise models. Experimental results conducted clearly that the proposed robust algorithm can well be applied on the any noise models (such as Noiseless, AWGN, Poisson Noise, Salt&Pepper Noise and Speckle Noise) at different noise power and the proposed algorithm can obviously improve the result in using both subjective and objective measurement.

6. Acknowledgement

This research work is a partial part of "VIDEO ENHANCEMENT USING AN ITERATIVE SRR BASED ON A ROBUST STOCHASTIC ESTIMATION WITH AN IMPROVED OBSERVATION MODEL" that has been supported by Research Grant for New Scholar (MRG5180263) from TRF (Thai Research Fund) and CHE (Commission on Higher Education) under Assumption University (Thailand).

7. References

Altunbasak, Y.; Patti, A.J.; and Mersereau, R.M. 2002. Super-resolution still and video reconstruction from MPEG-coded video. IEEE Trans. on Circuits and Systems for Video Technology 12(4): 217-26.

Black, M. J. and Rangarajan, A. (1996). On The Unification Of Line Processes, Outlier Rejection and Robust Statistics with Applications in Early Vision, International Journal of Computer Vision 19, 1 (July 1996): 57-92.

Elad, M. and Feuer, A. (1997). Restoration of a Single Superresolution Image from Several Blurred, Noisy and Undersampled Measured Images, IEEE Trans. on IP., 1997.

Elad, M. and Feuer, A. (1999a), Superresolution Restoration of an Image Sequence: Adaptive Filtering Approach, IEEE Trans. on IP., 1999.

Elad, M. and Feuer, A. (1999b). Super-Resolution Reconstruction of Image Sequences, IEEE Trans. on PAMI., vol. 21, Sep. 1999.

Elad, M. and Feuer, A. (1999c). Super-Resolution Restoration of Continuous Image Sequence – Adaptive Filtering Approach, Technical Report, The Technion, The Electrical Engineering Faculty, Israel Institute of Technology, Haifa, pp. 1-12.

Elad, M. and Hecov Hel-Or, Y. (2001). A Fast Super-Resolution Reconstruction Algorithm for Pure Translational Motion and Common Space-Invariant Blur, IEEE Trans. on IP., 2001.

Farsiu, S., Robinson, M. D., Elad, M., Milanfar, P. (2004), Advances and Challenges in Super-Resolution, Wiley Periodicals, Inc., 2004

Farsiu, S., Robinson, M. D., Elad, M. and Milanfar, P. (2004). Fast and Robust Multiframe Super Resolution, IEEE Transactions on Image Processing, Oct. 2004. pp. 1327-1344.

Farsiu, S., Elad, M. and Milanfar, P. (2006), Multiframe Demosaicing and Super-Resolution of Color Images, IEEE Transactions on Image Processing, Vol. 15, Jan. 2006, pp. 141-159.

He, Y., Yap, K., Chen, L. and Lap-Pui (2007). A Nonlinear Least Square Technique for Simultaneous Image Registration and Super-Resolution, IEEE Trans. on IP., Nov. 2007.

Kang, M. G. and Chaudhuri, S. (2003). Super-Resolution Image Reconstruction, IEEE Signal Processing Magazine, May. 2003.

Ng, M. K. and Bose, N. K. (2003), Mathematical analysis of super-resolution methodology, IEEE Signal Processing Mag., 2003.

Park, S. C., Park, M. K. and Kang, M. G. (2003). Super-Resolution Image Reconstruction : A Technical Overview, IEEE Signal Processing Magazine, Vol. 20, May 2003, pp 21-36.

Patti, A. J. and Altunbasak, Y. (2001). Artifact Reduction for Set Theoretic Super Resolution Image Reconstruction with Edge Constraints and Higher-Order Interpolation, *IEEE Trans. on Image Processing*, Jan. 2001

Rajan, D., Chaudhuri, S. and Joshi, M. V. (2003), Multi-objective super resolution concepts and examples, IEEE Signal Processing Magazine, Vol. 20, Issue 3, May. 2003, pp. 49-61

Rajan, D. and Chaudhuri, S. (2003), Simultaneous Estimation of Super-Resolution Scene and Depth Map from Low Resolution Defocuses Observations, IEEE Trans. PAMI., Sep. 2003

Schultz, R. R. and Stevenson R. L. (1994). A Bayesian Approach to Image Expansion for Improved Definition, IEEE Transactions on Image Processing, vol. 3, no. 3, May 1994, pp. 233-242.

Schultz, R. R. and Stevenson R. L. (1996). Extraction of High-Resolution Frames from Video Sequences, IEEE Transactions on Image Processing, vol. 5, no. 6, June 1996, pp. 996-1011.

Vorapoj Patanavijit received the B.Eng., M.Eng. and Ph.D. degrees from the Department of Electrical Engineering at the Chulalongkorn University, Bangkok, Thailand, in 1994, 1997 and 2007 respectively.
He has served as a full-time lecturer at Department of Computer and Network Engineering, Faculty of Engineering, Assumption University since 1998. He works in the field of signal processing and multidimensional signal processing, specializing, in particular, on Image/Video Reconstruction, SRR (Super-Resolution Reconstruction), Enhancement, Fusion, Denoising, Inverse Problems, Motion Estimation and Registration.

Fig. 3. The Experimental Result of Proposed SRR Algorithm: Lena
(The bottom image on our experiment result of each subfigure is the absolute difference between it's correspond top image to the original HR image. The difference is magnified by 5.)

Fig. 3. The Experimental Result of Proposed SRR Algorithm: Lena (Cont.)
(The bottom image on our experiment result of each subfigure is the absolute difference between it's correspond top image to the original HR image. The difference is magnified by 5.)

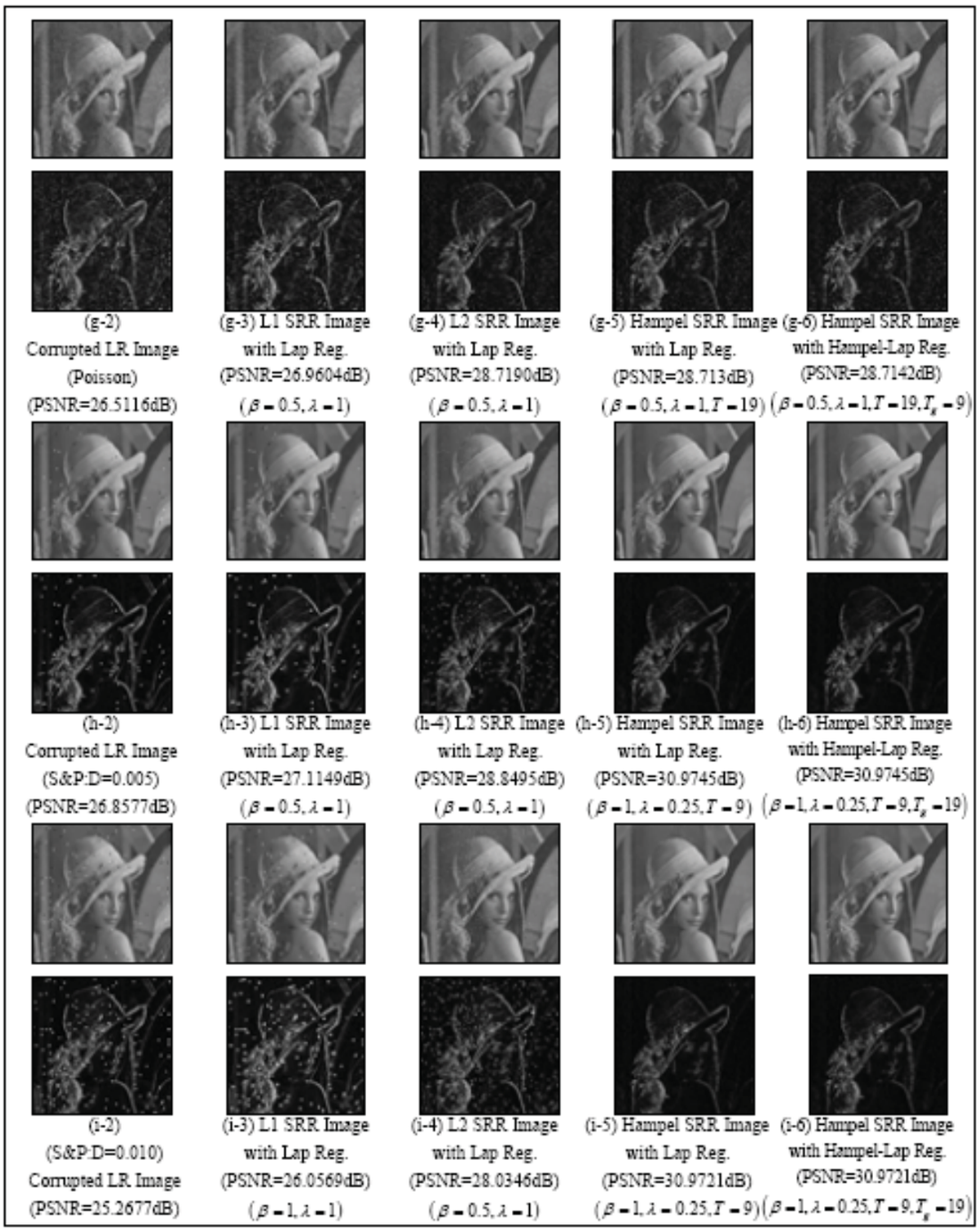

Fig. 3. The Experimental Result of Proposed SRR Algorithm: Lena (Cont.)
(The bottom image on our experiment result of each subfigure is the absolute difference between it's correspond top image to the original HR image. The difference is magnified by 5.)

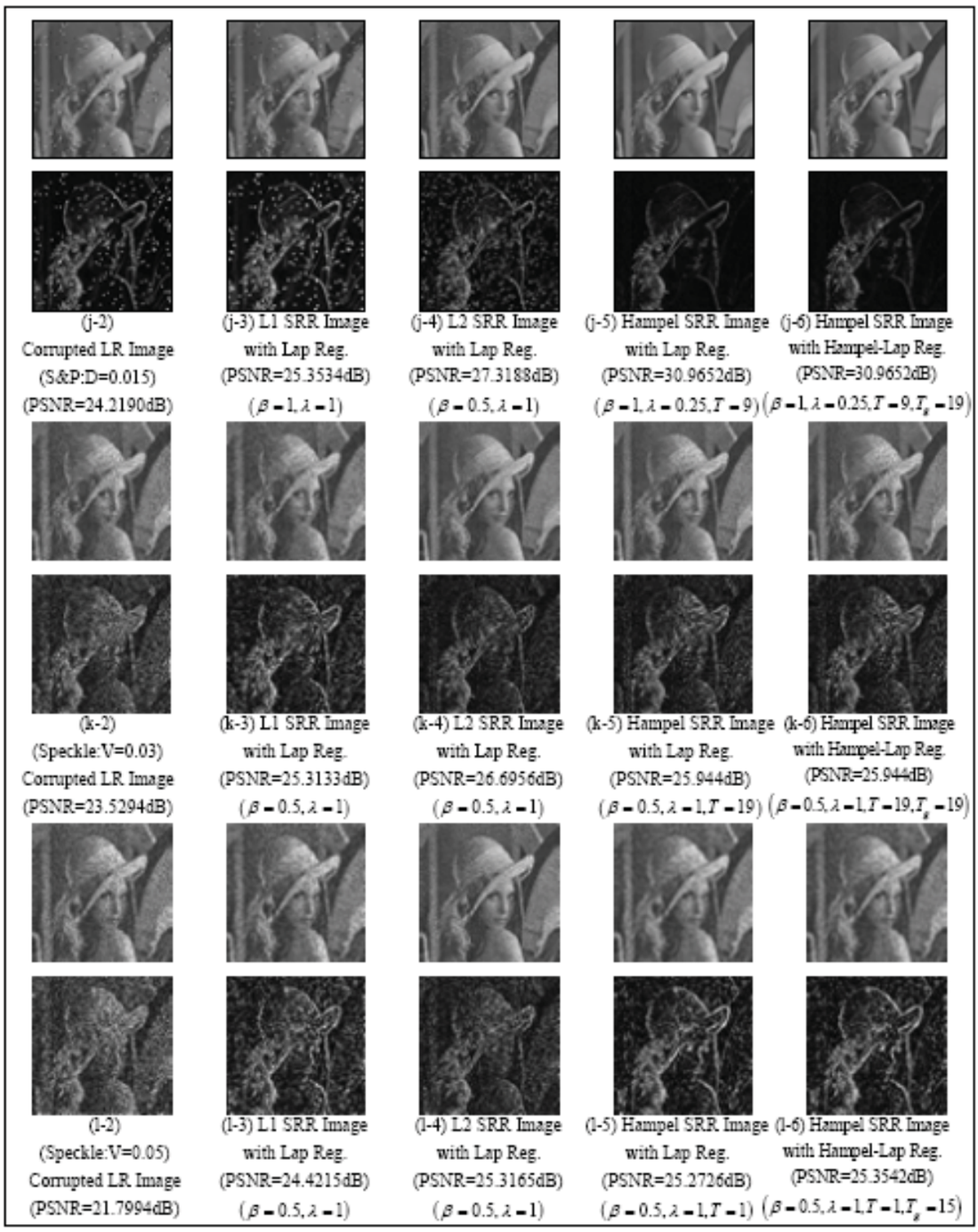

Fig. 3. The Experimental Result of Proposed SRR Algorithm: Lena (Cont.)
(The bottom image on our experiment result of each subfigure is the absolute difference between it's correspond top image to the original HR image. The difference is magnified by 5.)

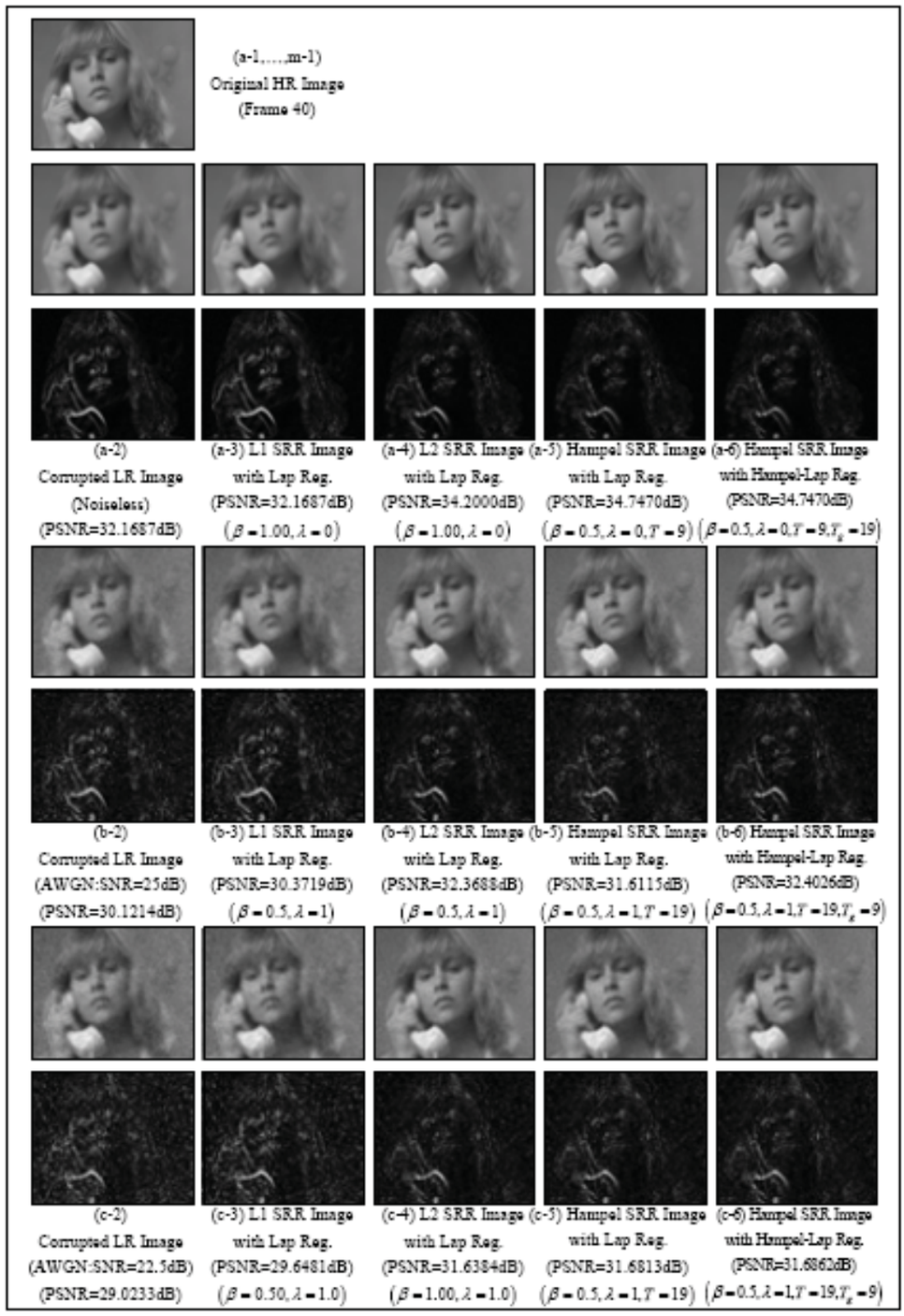

Fig. 4. The Experimental Result of Proposed SRR Algorithm: Susie (40th Frame)
(The bottom image on our experiment result of each subfigure is the absolute difference between it's correspond top image to the original HR image. The difference is magnified by 5.)

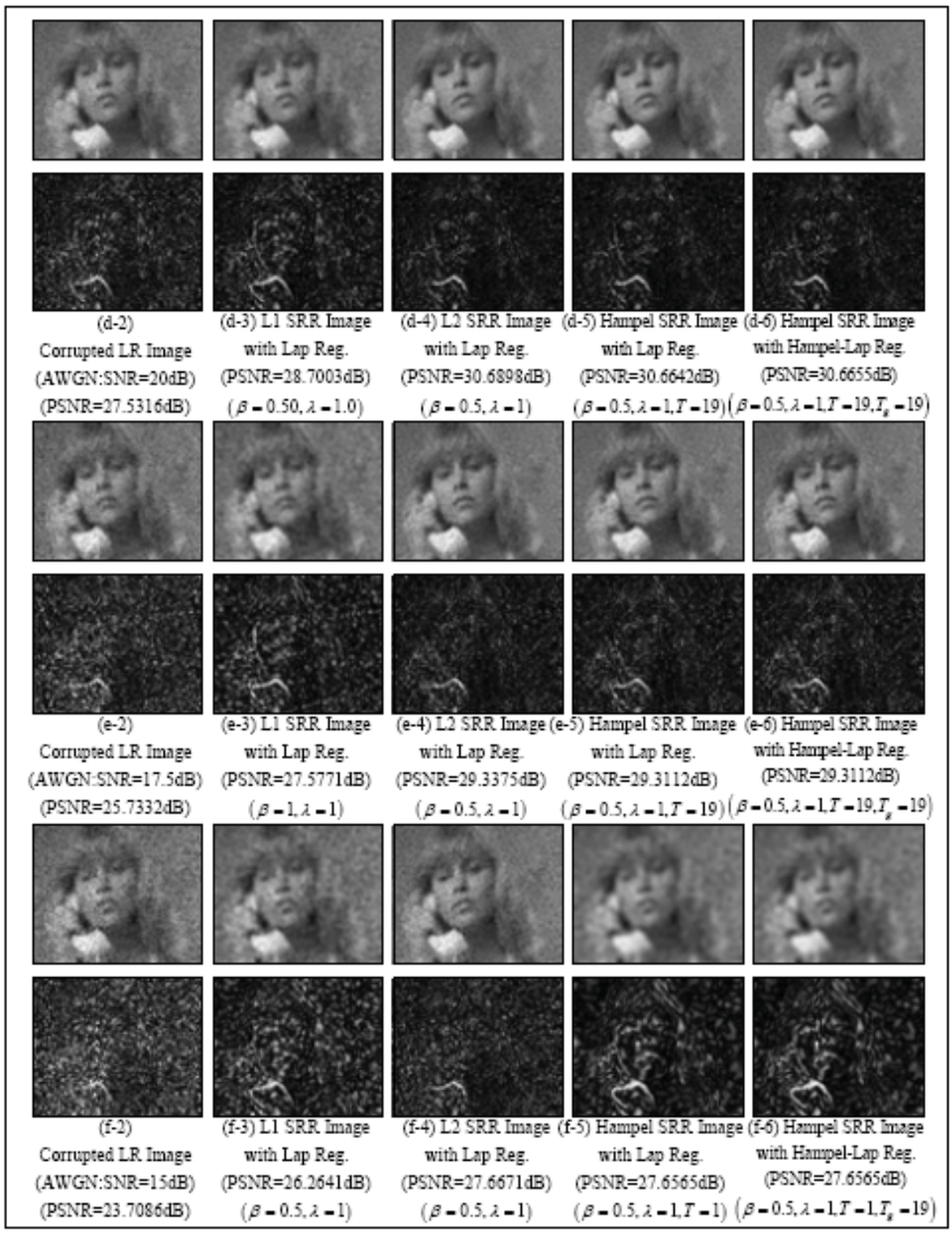

Fig. 4. The Experimental Result of Proposed SRR Algorithm: Susie (40th Frame) (Cont.)
(The bottom image on our experiment result of each subfigure is the absolute difference between it's correspond top image to the original HR image. The difference is magnified by 5.)

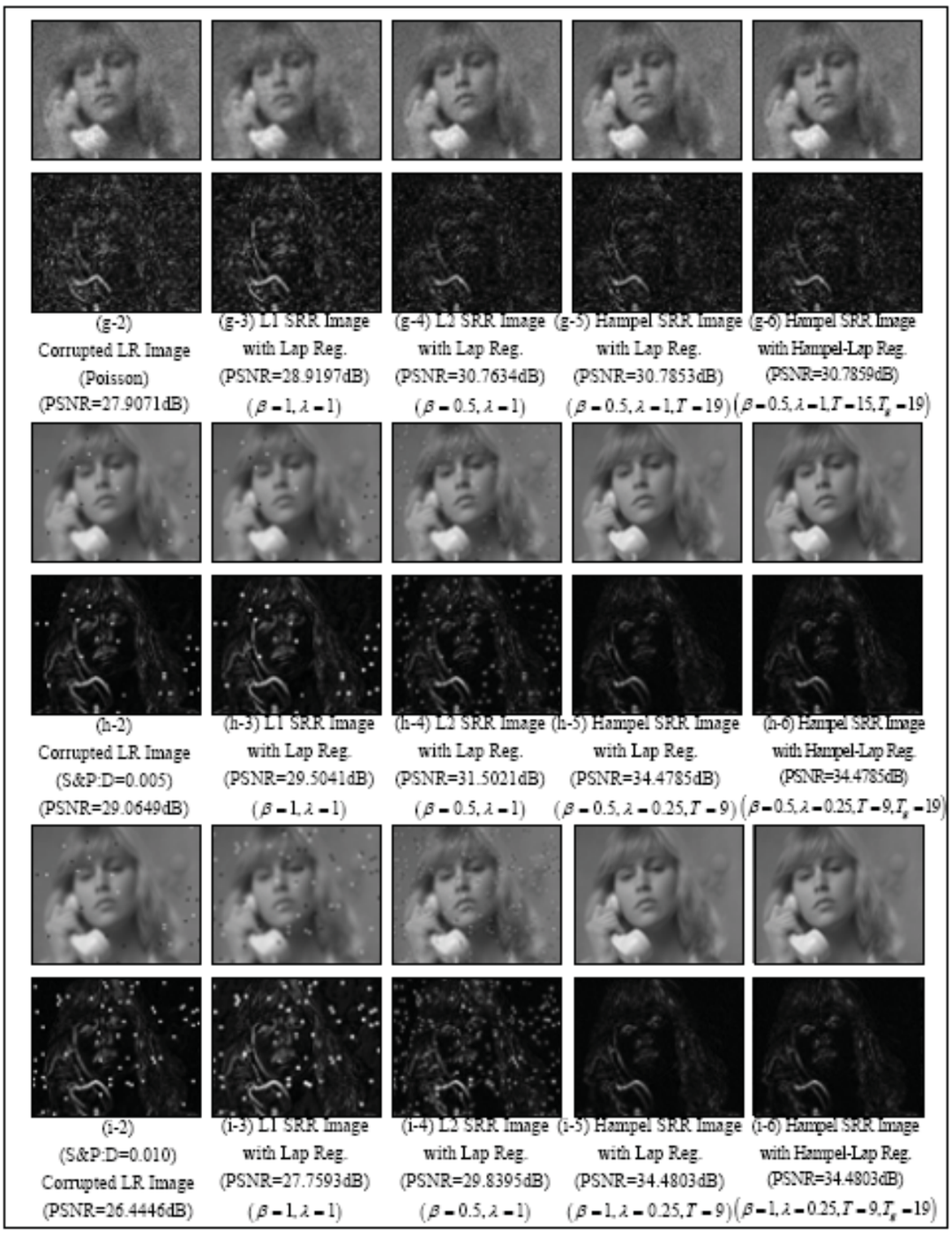

Fig. 4. The Experimental Result of Proposed SRR Algorithm: Susie (40th Frame) (Cont.)
(The bottom image on our experiment result of each subfigure is the absolute difference between it's correspond top image to the original HR image. The difference is magnified by 5.)

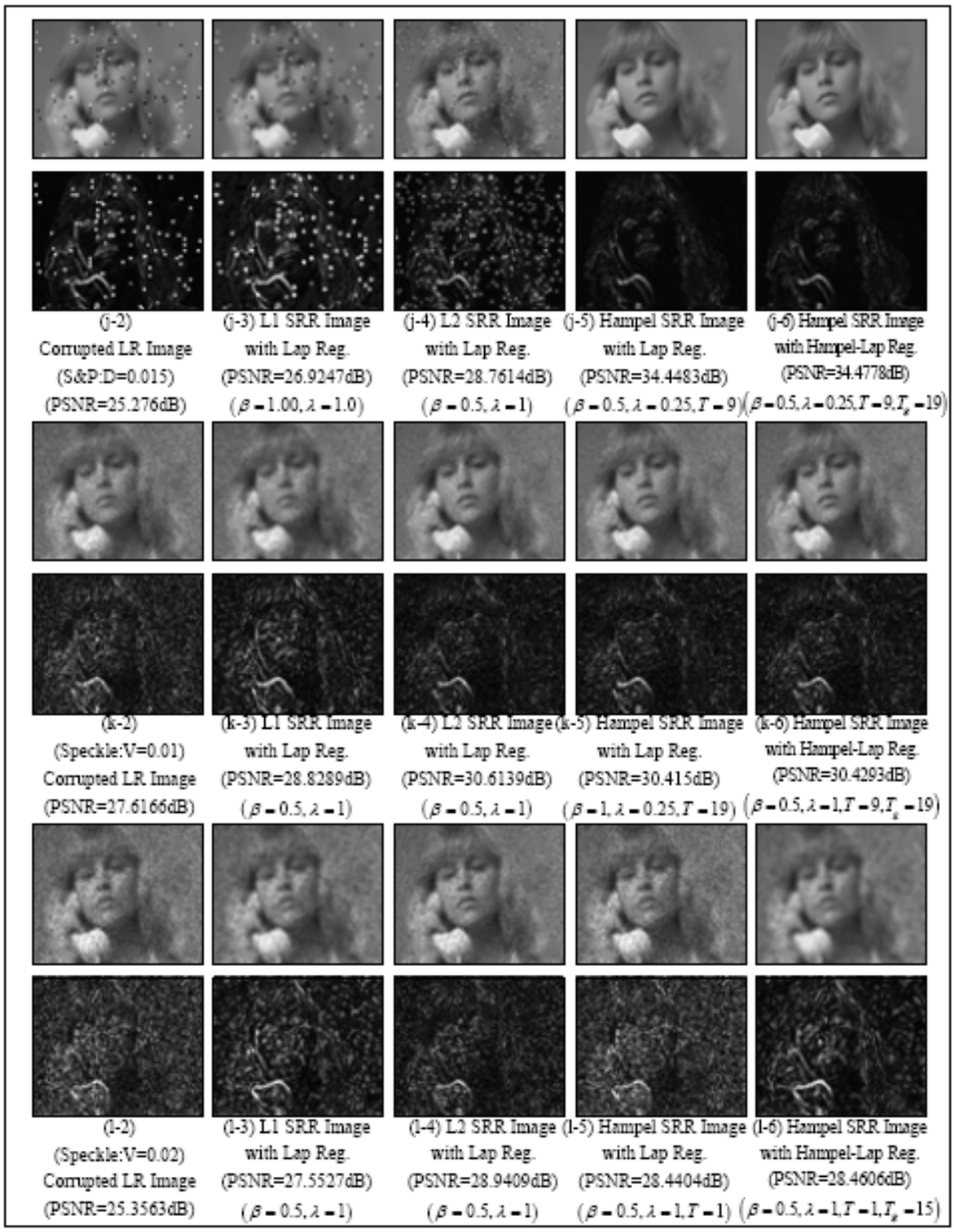

Fig. 4. The Experimental Result of Proposed SRR Algorithm: Susie (40th Frame) (Cont.)
(The bottom image on our experiment result of each subfigure is the absolute difference between it's correspond top image to the original HR image. The difference is magnified by 5.)

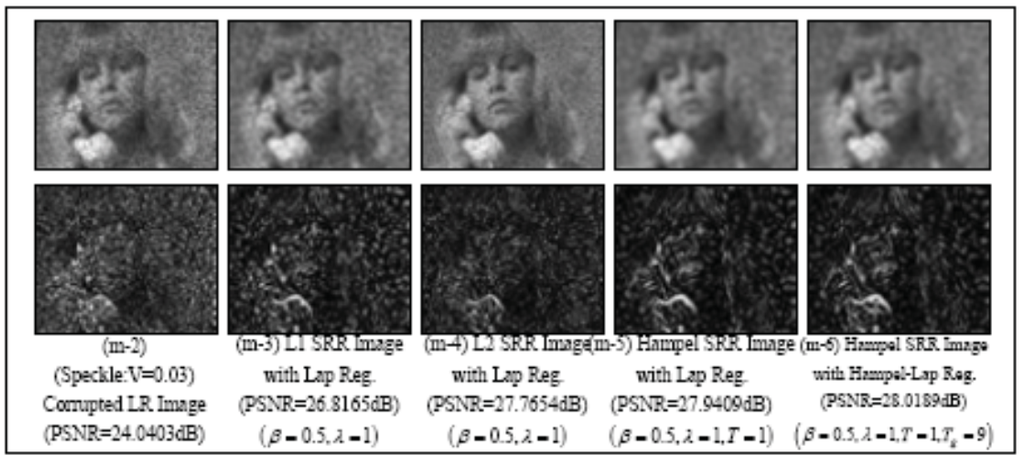

Fig. 4. The Experimental Result of Proposed SRR Algorithm: Susie (40th Frame) (Cont.)
(The bottom image on our experiment result of each subfigure is the absolute difference between it's correspond top image to the original HR image. The difference is magnified by 5.)

IntechOpen

Pattern Recognition
Edited by Peng-Yeng Yin

ISBN 978-953-307-014-8
Hard cover, 568 pages
Publisher InTech
Published online 01, October, 2009
Published in print edition October, 2009

For more than 40 years, pattern recognition approaches are continuingly improving and have been used in an increasing number of areas with great success. This book discloses recent advances and new ideas in approaches and applications for pattern recognition. The 30 chapters selected in this book cover the major topics in pattern recognition. These chapters propose state-of-the-art approaches and cutting-edge research results. I could not thank enough to the contributions of the authors. This book would not have been possible without their support.

How to reference
In order to correctly reference this scholarly work, feel free to copy and paste the following:

Vorapoj Patanavijit (2009). A Robust Iterative Multiframe SRR Based on Hampel Stochastic Estimation with Hampel-Tikhonov Regularization, Pattern Recognition, Peng-Yeng Yin (Ed.), ISBN: 978-953-307-014-8, InTech, Available from: http://www.intechopen.com/books/pattern-recognition/a-robust-iterative-multiframe-srr-based-on-hampel-stochastic-estimation-with-hampel-tikhonov-regular

INTECH
open science | open minds

InTech Europe
University Campus STeP Ri
Slavka Krautzeka 83/A
51000 Rijeka, Croatia
Phone: +385 (51) 770 447
Fax: +385 (51) 686 166
www.intechopen.com

InTech China
Unit 405, Office Block, Hotel Equatorial Shanghai
No.65, Yan An Road (West), Shanghai, 200040, China
中国上海市延安西路65号上海国际贵都大饭店办公楼405单元
Phone: +86-21-62489820
Fax: +86-21-62489821

© 2009 The Author(s). Licensee IntechOpen. This chapter is distributed under the terms of the Creative Commons Attribution-NonCommercial-ShareAlike-3.0 License, which permits use, distribution and reproduction for non-commercial purposes, provided the original is properly cited and derivative works building on this content are distributed under the same license.

IntechOpen

IntechOpen